ELSEVIER

Journal of Hazardous Materials 142 (2007) 720–729

Journal of Hazardous Materials

www.elsevier.com/locate/jhazmat

LNG pool fire spectral data and calculation of emissive power

Phani K. Raj *

Technology & Management Systems, Inc., 102 Drake Road, Burlington, MA 01803, USA

Available online 6 July 2006

Abstract

Spectral description of thermal emission from fires provides a fundamental basis on which the fire thermal radiation hazard assessment models can be developed. Several field experiments were conducted during the 1970s and 1980s to measure the thermal radiation field surrounding LNG fires. Most of these tests involved the measurement of fire thermal radiation to objects outside the fire envelope using either narrow-angle or wide-angle radiometers. Extrapolating the wide-angle radiometer data without understanding the nature of fire emission is prone to errors. Spectral emissions from LNG fires have been recorded in four test series conducted with LNG fires on different substrates and of different diameters. These include the AGA test series of LNG fires on land of diameters 1.8 and 6 m, 35 m diameter fire on an insulated concrete dike in the Montoir tests conducted by Gaz de France, a 1976 test with 13 m diameter and the 1980 tests with 10 m diameter LNG fire on water carried out at China Lake, CA. The spectral data from the Montoir test series have not been published in technical journals; only recently has some data from this series have become available. This paper presents the details of the LNG fire spectral data from, primarily, the China Lake test series, their analysis and results. Available data from other test series are also discussed.

China Lake data indicate that the thermal radiation emission from 13 m diameter LNG fire is made up of band emissions of about 50% of energy by water vapor (band emission), about 25% by carbon dioxide and the remainder constituting the continuum emission by luminous soot. The emissions from the H_2O and CO_2 bands are completely absorbed by the intervening atmosphere in less than about 200 m from the fire, even in the relatively dry desert air. The effective soot radiation constitutes only about 23% during the burning period of methane and increases slightly when other higher hydrocarbon species (ethane, propane, etc.) are burning in the LNG fire.

The paper discusses the procedure by which the fire spectral data are used to predict the thermal emission from large LNG fires. Unfortunately, no direct measurements of the soot density or smoke characteristics were made in the tests. These parameters have significant effect on the thermal emission from large LNG fires.

Keywords: LNG fire; Spectrum; Surface emissive power; Thermal radiation; Spectral radiance; Soot emissivity; Band emission; Atmospheric absorption

1. Background

In the 1970s there was considerable interest in assessing the potential hazards arising from accidental releases of liquefied natural gas (LNG) during its shipment and/or storage in terminals. One concern was the effect of combustion of the released LNG on the surrounding area (people and structures), and the distances up to which the hazardous effects of thermal radiation from such fires would persist. Extensive tests were conducted in the US, Europe and Japan to study various aspects of LNG releases, the types of hazards posed, and the characteristics of these hazards, especially the burning rates of and hazardous distances from LNG fires. A review of the tests conducted up to 1981 and summary of the findings there from have been published by GRI [1]. Because of the expected substantial increase in the importation of LNG into the US in the coming decade and the number of application pending before the Federal Energy Regulatory Commission (FERC) for permits to construct LNG receiving terminals and storage facilities (some of them close to population centers), there is renewed public debate on LNG safety. In addition to the concerns of accidental releases the possibility of LNG transportation and storage infrastructure being the targets of terrorist attack has escalated the debate over LNG hazards and the extent of these hazards. One of the prime hazardous events debated and discussed in technical literature is the occurrence of a large LNG pool fire and the extent of its hazardous effects [2].

While there have been a number of technical papers in the literature discussing the various aspects of a LNG pool fire [3,4]

Abbreviations: AGA, American gas association; SEP, surface emissive power (of the fire); LNG, liquefied natural gas

* Tel.: +1 781 229 6119.
E-mail address: tmsinc1981@verizon.net.

0304-3894/$ – see front matter © 2006 Elsevier B.V. All rights reserved.
doi:10.1016/j.jhazmat.2006.06.130

to date there have been no technical publications related to the spectral emission characteristics of LNG fires. An understanding of the infrared (radiation) emission spectrum for a fire provides a means by which several characteristics of the fire can be inferred, namely, the distribution of energy radiated in different wavelengths or bands, emission from soot, density of luminous soot, flame emission temperature, partial pressures of water vapor and carbon dioxide in the fire, etc. The knowledge of the total irradiance from the fire and the energy distribution in various wave lengths can be utilized, along with the understanding of the wave-length sensitive absorption characteristics of the intervening atmosphere, to calculate the total heat flux received by an object at different distances from the fire. Also the skin burn hazard to people will depend on the wavelength-dependent thermal absorption characteristics of the skin and the wavelength of the incident radiation.

The author is aware of at least four sets of field experiments in which the spectral characteristics of LNG fires were measured, namely, (i) in the American gas association sponsored AGA [5] LNG fire tests, (ii) in a single test of the China Lake LNG fire-on-water test series of 1976 [6], (iii) the pool fire tests in China Lake in 1980 [7], and (iv) in the 1987 Montoir LNG fire tests on insulated concrete [8]. The results from the AGA tests were determined to be unreliable since a very slow scanning grating type spectrometer was used; hence the spectra measured were severely affected by intensity fluctuation in the flame. The spectral measurements from a single test in the 1976 China Lake test series are documented in detail. Limited data are available from the 1980 tests. Data from the 1987 Montoir tests have not been published. The objective of this paper is to provide the details of spectral measurements made in the AGA tests, 1976 China Lake tests, and the limited results from the 1987 tests.

2. Introduction

Generally, a fire is a band emitter with a superposed continuum emission due to luminous soot. In order to obtain the total emission the location of the spectral bands and the emissivity in these bands are needed. Also it is important to know the temperature of emission. The radiation emitted by the fire is absorbed in the atmosphere. To calculate the net radiant heat received by an object located outside the fire it is important to know the emission characteristics of the fire as well as the absorption characteristics of the atmosphere in addition to the path length through the atmosphere.

The principal products that result from the combustion of stoichiometric proportions of methane and air are water vapor (H_2O) and carbon dioxide (CO_2). However, in a real LNG fire methane is not the only constituent that is burning and not all of the combustion occurs at stoichiometric proportions. Also not all of the (fuel) pyrolysis products get burned completely. In fact, the reason that the fire is visible at all is due to the presence of soot particles that glow at the fire temperature and emit continuous radiation at all wavelengths. Hence, the radiant emission from a LNG fire will be from H_2O vapor, CO_2, CO, unburned (and heated) CH_4, and other intermediate reaction products. It is estimated that the dominant species from which radiation is emitted are the H_2O, CO_2 and the luminous soot particles. In large LNG fires (greater than about 35 m diameter), formation of cold smoke begins to occur and this has effect on the radiation output from the fire to external objects. This phenomenon has been discussed in another recent paper by Raj [4] and is not the subject of this article. In this paper the spectral emission measurements from relatively small size LNG fires (about 15 m diameter) are discussed.

Table 1
Infrared emission bands from molecular species in combustion gases

Gas	Principal bands centered at wavelengths, λ_B (μm)	Remarks
H_2O	1.88, 2.66 and 6.27	Strong emission/absorption bands
	0.94, 1.14, 1.38, 2.74 and 3.17	Weak emission/absorption bands
CO_2	2.69, 2.77 and 4.26	Strong emission/absorption bands
	1.96, 2.01, 2.06, 4.68, 4.78 and 4.82	Weak emission/absorption bands
CO	1.573, 2.345 and 4.663	
HCl	1.198, 1.764 and 3.465	
NO	2.672 and 5.3	Weak emission/absorption bands
NO_2	4.5, 6.17 and 15.4	
N_2O	2.87, 3.9, 4.06, 4.54, 7.78, 8.57 and 16.98	
SO_2	4.0, 4.34, 5.34, 7.35 and 8.69	

Source: Wolfe [10].

The principal emission (and, therefore, also absorption) bands for water vapor, CO_2 and other species that occur in combustion gases are indicated in Table 1. The magnitude of emission/absorption depends upon the "width" of the absorption band; the higher the temperature, the higher the bandwidth centered about the principal wavelengths shown in Table 1. A useful concept for quick estimation of the absorption of a continuum emission (such as from a black body) by the molecules in the atmosphere is the "equivalent bandwidth of complete absorption." The energy absorbed per unit solid angle is given by the integral of the product of the black body spectral radiant intensity (I_λ in W/sr μm), spectral absorptivity (α_λ) and dλ over the band of interest. The ratio of this energy absorbed and the radiant intensity at the principal absorption wavelength (λ_B) is termed the equivalent bandwidth for complete absorption ($\Delta\lambda$) expressed in units of wavelength (μm). The equivalent bandwidth for complete absorption has been calculated by Raj et al. [6] for three absorption bands, in the wavelength range of interest (1.5 μm through 5.5 μm). These are indicated in Table 2 for water vapor and Table 3 for carbon dioxide. Also shown in these tables are the fractional absorptions of energy radiated by a black body at 1300 K by the atmospheric gases for different path lengths through the atmosphere.

3. Measured spectral data from LNG pool fires

Tests of LNG fires on soil dikes (of 1.8 and 6 m diameter) were conducted in 1972–1973 under the sponsorship of the American gas association, AGA [5]. Spectral measurements were made with a very slow scanning, grating type, spectrometer located,

Table 2
Thermal radiation absorption band widths for two principal H_2O (vapor) bands (for different atmospheric path lengths at 300 K and 50% RH)

Path length through the atmosphere (m)	Precipitable water layer thickness (mm)	1.87 μm band		2.7 μm band	
		Total absorption band width, Δλ (μm)	Fraction of the energy emission from a 1300 K black body absorbed (μm)	Total absorption band width, Δλ (μm)	Fraction of the energy emission from a 1300 K black body absorbed
400	5	0.16	0.04	0.58	0.16
160	2	0.12	0.03	0.51	0.14
80	1	0.10	0.03	0.45	0.12
8	0.1	0.03	0.01	0.22	0.06
0.8	0.01	0.01	0.003	0.07	0.02

respectively, at 14 m from the 1.8 m fire, and 36.6 m from the 6 m fire. Because of the slowness of the spectrometer the recorded spectra were reported to have been severely affected by intensity fluctuation in the flame. The data presented therefore may not be reliable. Unfortunately additional details of the characteristics or the accuracy of the spectrometer used in these AGA tests are unavailable.

In the period 1976–1978 several LNG pool fires-on-water tests were conducted in China Lake. All tests involved the LNG spill on to water surface at the center of a 50 m × 60 m × 1 m depth, man-made, spring fed pond. All spills were ignited either immediately or slightly delayed, to form pool fires on water. In one of the tests (test #5 of 10 July 1976) the fire thermal radiation emission was measured by a fast scanning Michelson interferometer located at 236 m from the spill point mounted on a truck. The detector lens and the mask on the face of the detector defined the field of view of the instrument to a 6° full cone angle. The detector was a liquid nitrogen cooled InSb diode and the beam splitter was made of KBr. The spectrometer had two Irtran 2 windows and two PbSe field lenses. Before use in the field the spectrometer had been calibrated against a black-body source at 1116 K. The theoretical spectral radiance from the black body and the measured spectral radiance agreed extremely closely. The choice of the detector limited the interferometer to wavelengths less than 5.5 μm. The spectral wavelengths from 1.5 to 5.5 μm were scanned with 7.7 cm^{-1} resolution. The data obtained from different scans have been reduced at approximately 5 s intervals with the first scan starting at 5.4 s after the ignition of the LNG pool.

Table 3
Thermal radiation absorption band widths for the principal CO_2 band (for different atmospheric path lengths at 300 K)

Path length through the atmosphere (m)	4.3 μm band	
	Total absorption band width, Δλ (μm)	Fraction of the energy emission from a 1300 K black body absorbed
1000	0.28	0.04
236	0.24	0.03
100	0.22	0.03
10	0.17	0.02
1	0.065	0.01
0.3	0.033	0.004

The spectrometer used in test #5 of China Lake test series was located 236 m from the spill point and was aimed at about 4 ± 1 m above the water surface. The shape and size of the visible LNG pool fire at about 20 s into the burn and the field of view of the spectrometer are shown in Fig. 1. It is noted that the field of view of the spectrometer is not completely filled by the fire. The spectrometer view area at the location of the fire is 481 m^2 whereas the actually "seen" (projected) fire area is 213 m^2; i.e., only about 44.3% of the spectrometer field is filled with the image of the fire. It is also noted that the spectrometer "sees," in addition to the direct emission from the fire, some reflected emission from the water surface. However, the reflected energy received is calculated to be small compared to the total energy received because of the comparatively small flame area seen in the reflection and because the reflection may not be perfect (due to the waves on water surface). Also, IR reflection by water in the 1–6 μm band is estimated to be 20% (with the exception of a peak of 40% at 3 μm). Hence, no correction has been made in

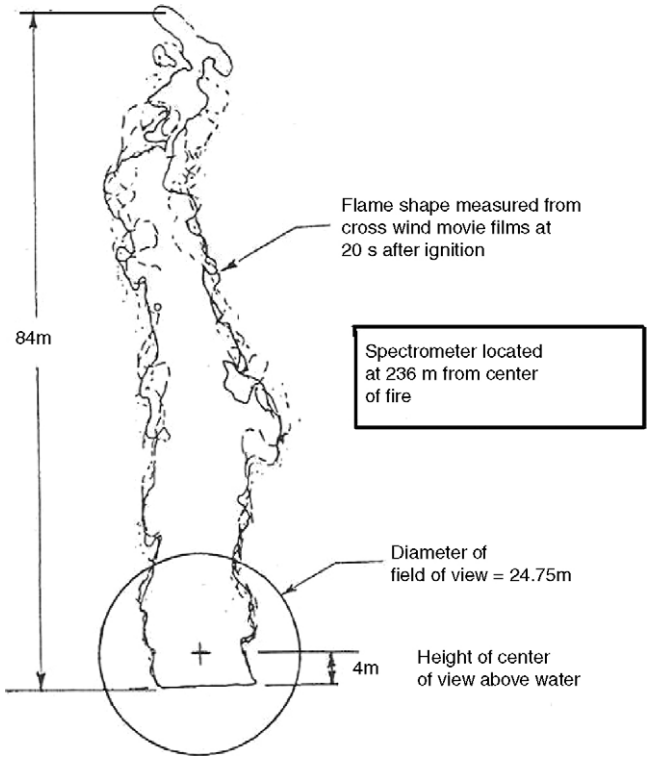

Fig. 1. Field of view of spectrometer in China Lake test #5.

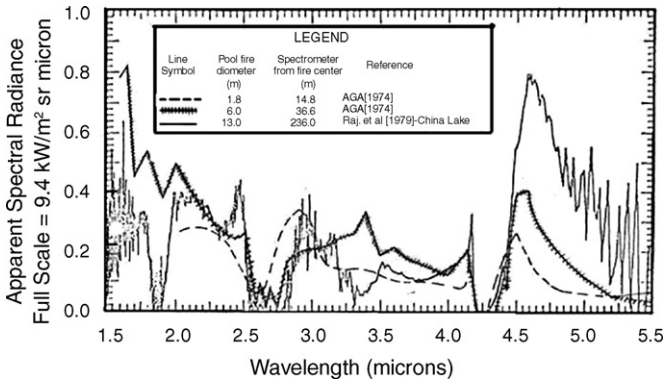

Fig. 2. Typical LNG pool fire spectra from AGA tests and in China Lake test #5 at 20 s.

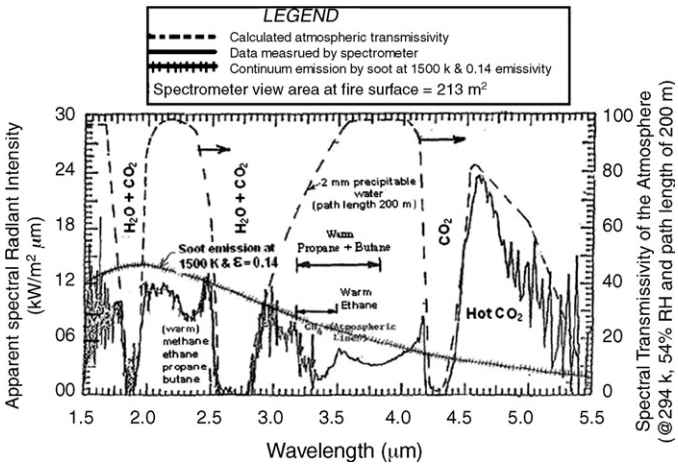

Fig. 3. Observed LNG fire spectrum at 20 s and calculated soot emission and atmospheric spectral transmissivity.

the data to account for the reflected energy. Details of the spectrometer calibration with the blackbody radiation, determination of the units of full scale of spectrometer output (in kW/sr μm), and calculation of the conversion factor for interpreting the spectrometer output in terms of apparent spectral radiant intensity at the fire surface (knowing the location of the spectrometer and its field of view) are indicated by Raj et al. [6].

Twelve (12) representative spectra were reduced from the China Lake test data, at about 5 s intervals. The duration of intense fire in this test lasted about 26 s; spectral data continued to be measured beyond the period of intense burning. Fig. 2 shows the data obtained from a typical scan in the China Lake tests [6] as well as the spectral data measured in the AGA tests [5]. The abscissa (*X*-axis) represents the wavelength of thermal radiation in the region of interest. The ordinate (*Y*-axis) represents the "apparent spectral radiant intensity" of the fire. This value is "apparent" because the data presented in Fig. 2 has not been corrected for the absorption of radiation in the intervening atmosphere. The AGA data also has been plotted to the same scale. The actually seen flame area is used to convert the measured intensity at the spectrometer into the spectral radiance value shown on the *Y*-axis of Fig. 2.

Fig. 2 shows the atmospheric absorption of the radiation in the 1.87 μm and 2.7 μm water bands and by the 4.3 μm CO_2 band. The measured distribution of apparent spectral radiance of the fire has no resemblance to that from a blackbody emitter, I_λ (see foot note below).[1] This is not merely due to the atmospheric and other absorption spectra superposed on the blackbody spectral radiance but is chiefly due, in large part, to the band emissions from gaseous species, chiefly H_2O and CO_2. The remainder of the total emission originates from luminous soot particles. An analysis of the results in Fig. 2 indicates the following:

1. Comparison of the spectra from two completely different test series indicates certain commonalities as well as differences. The spectra from both test series indicate the "absorption wells" due to water vapor and CO_2 absorption in the atmosphere of the emissions from the fire in the same (H_2O and CO_2) bands.
2. The apparent spectral radiance in wavelengths less than 4.5 μm seems to be higher in the 6 m AGA fire than in the 13 m China Lake fire. If the atmospheric absorption is taken into account (properly) then the true flame spectral radiance will be higher for the China Lake fire, as can be expected, because of the larger optical path length to the spectrometer in the latter fire.
3. The absorption in 4.3–5.5 μm CO_2 band seems to be much smaller in the 236 m path length of the China Lake test than in the shorter path lengths of the AGA tests. This result is certainly anomalous and is perhaps due to the instrument errors and inefficiencies in the AGA tests. The results from China Lake tests are more acceptable because of better calibration techniques and accuracy of the instrument used in the test. Henceforth, all discussions of the data are with the results obtained from China Lake test #5.

The calculation of the spectral transmissivity of the atmosphere is a tedious job. Atmospheric absorption tables for different path lengths, spectral bands and humidity conditions are available in Wolfe [10]. Using these values the wavelength dependent transmissivity for a 294 K and 54% relative humidity atmosphere for a path length of 200 m (i.e., 2.3 mm precipitable water vapor) has been calculated. Details are presented by Raj et al. [6]. This calculated atmospheric transmissivity is plotted as a function of the wavelength in Fig. 3 superposed on the spectrum measured at 20 s into the fire burn. In Fig. 3 the *Y*-axis represents the spectral radiant intensity (also known in the literature as "spectral emissive power"). Different absorption bands and the molecular species contributing to the absorption are also indicated. Also shown in Fig. 3 is the (calculated) continuous emission spectrum from a grey body at temperature 1500 K and of emissivity (ε) 0.14; this spectrum is attributed to lumi-

[1] The blackbody spectral radiant emittance (E_λ) is given by Hottel and Sarofim [9], $E_\lambda = \pi I_\lambda$ and $I_\lambda = (2hc^2n^2\lambda^{-5})/\{e^{hc/k\lambda T} - 1\}$ where, c is the velocity of light = 2.9979×10^8 (m/s); E_λ the Spectral radiant emittance = πI_λ (W/m² m); h the Planck constant = 6.6256×10^{-34} (J s); I_λ the Blackbody spectral radiance (W/sr m² m); k the Boltzmann constant = 1.3805×10^{-23} (J/K); n the refractive index = 1 for air; T the temperature of the blackbody (K); and λ is the wavelength of radiation (m). The integration of the spectral radiant emittance (E_λ) over the entire emission wavelength in the IR region of the electromagnetic spectrum gives the "emissive power" (E) of the fire.

nous soot (see discussions in a later section). The true spectral radiance of the fire is the sum of the true radiance due to the soot together with the band emission from H_2O and CO_2 bands. The following additional observations are made from the results shown in Fig. 3.

1. The spectrum in the 1.5–1.75 μm is noisy; but the mean level of the spectral radiance can be interpreted as due to luminous soot. In Fig. 3 the calculated continuum emission from luminous soot at 1500 K and with an emissivity of 0.14 is indicated. These values for soot emission were chosen to match the maximum measured soot radiance of 910 kW/sr μm measured at 2.15 μm wavelength (where the atmospheric absorption from water vapor and CO_2 is essentially zero).
2. The 1.75–2 μm region is dominated by the 1.87 μm water (and overlapping CO_2) absorption band. The shape of the spectrum agrees with known atmospheric spectra. According to Wolfe [10], the equivalent total absorption bandwidth at 1.87 is 0.12 μm. In fact, it is seen from the data that the totally absorbed band has a width about his value.
3. In the 2–2.6 μm range there are no band emissions from water vapor or CO_2. The observed spectral signal is therefore due to luminous soot emissions only. Also, as shown in Fig. 3, the atmospheric transmissivity is essentially 1 in this wavelength range (for the 200 m distance used in the transmissivity calculations). However, the observed spectrum shows absorption. This is assumed to be due to absorption by unburnt, relatively warm, hydrocarbon vapor molecules (methane, ethane, propane, butane, etc.) close to the base of the fire at which the spectrometer view was focused.
4. The 2.6–4.3 μm region is dominated by the (total) absorption by water vapor band at 2.66 μm. The calculated water vapor absorption bandwidth (for the 2 mm precipitable water in the 200 m distance) is 0.5 μm and will be between 2.41 and 2.91 μm. The actually observed "well" is only between 2.55 and 2.75 μm with intensity spikes at both ends. It is estimated that these spikes are due to emission from the hot water vapor in the fire, which is only partially absorbed by the "cold" water vapor in the atmosphere due to the fact that the spectral lines of hot and cold water vapor due not precisely coincide.
5. The sharp lines at 3.2 and 3.3 μm are attributed to methane vapors surrounding the fire due to LNG vaporization. Also noticed in the 3.3–3.5 μm the intensity is bottomed and there is no fine structure in the line. This is attributed to the total absorption of soot radiation in this region and emission from warm hydrocarbon gases (of ethane, propane an butane that are optically thick.
6. The region between 3.5 and 4 μm is interesting in that no line structure is exhibited. (It is noted that the accuracy of spectral measurement is 7.7 cm^{-1} or 1.12×10^{-2} μm; hence, if any fine structure were recorded they would be exhibited in the data. None are shown, however.) The calculated atmospheric transmissivity in this region is 40%, the primary absorptions are due to cold hydrocarbon gases (possibly in the atmosphere outside the fire).
7. The spike at 4.15 μm is due to the hot CO_2 emission line from the fire not absorbed by the cold CO_2 in the atmosphere.
8. The 4.3–5.5 μm region. In this spectral region much of the emission by hot CO_2 and CO in the flame is absorbed by the cold CO_2 in the atmosphere. The calculated bandwidth for the 236 m path length through the atmosphere for the CO_2 absorption is 0.24 μm. Hence, any CO_2 emission from the flame in the 4.18–4.42 μm should be absorbed completely, as is indeed seen in the spectral data shown in Fig. 3. The total bandwidth for CO_2 emission from the flame at 4.3 μm is dependent on the flame temperature and the partial pressure, beam length product. Neither of these quantities was directly measured. However, it can be argued that the emission bandwidth at flame temperature is much larger than the atmospheric absorption bandwidth. Hence, some of the CO_2 emission from the fire will get through the atmosphere. This is indeed observed with a peak recorded at 4.6 μm. The thermal emission spectrum from the vibrational band of hot CO_2 is distorted considerably by water vapor in the atmosphere, beyond about 4.5 μm. From 4.7 μm, a strong water absorption band with a resolved line spectrum begins. The atmosphere becomes completely opaque at about 5.5 μm. According to Plass [10] this water band is strong enough to be opaque even at water concentrations much below 1 mm of precipitable water in the atmosphere. Radiation in this wavelength range will be completely absorbed in tens of meters rather than in hundreds of meters.
9. The 5.5–25 μm region: no spectral measurements were made in this wavelength space. The fraction of a blackbody emitted total energy that lies in this region varies between 26% at 1100 K to about 14% at 1500 K; hence, their contribution to the overall emissive power calculations from measured spectra can be considered to be small. The opaque region extends from 5.4 up to 7.4 μm. An important CO_2 absorption band occurs at 15 μm. In addition, there are two significant water absorption bands at 20 and 23 μm and total absorption beyond 23 μm.

Fig. 5 shows a similar spectrum from the lower regions of a 35 m diameter LNG fire on insulated concrete dike [11]. The *Y*-axis of this figure is also in spectral radiant intensity units so

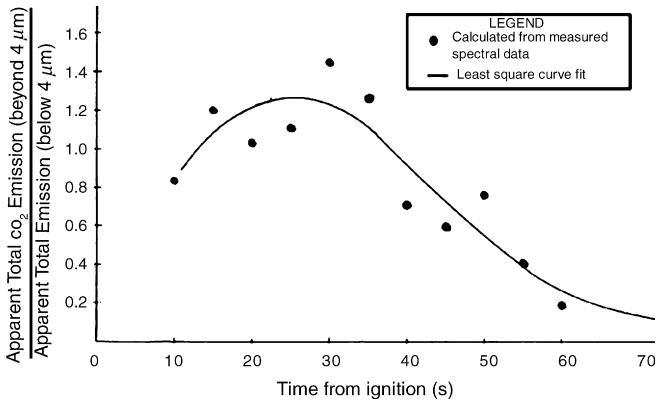

Fig. 4. Relative emissions from CO_2 and luminous soot as a function of burn time.

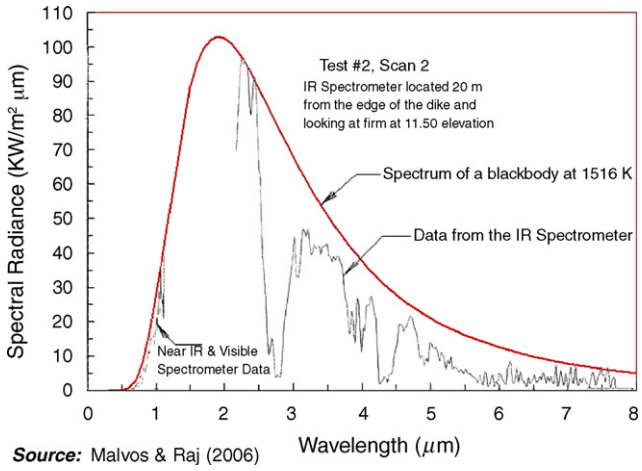

Fig. 5. Blackbody spectrum at 1516 K vs. spectral data from a 35 m diameter LNG fire on insulated concrete dike.

that the results can be compared directly with those in Fig. 3. The spectrum was measured at a distance of 20 m from the edge of the dike (fire boundary) by nitrogen purged, highly insulated spectrometers, one sensitive to the visible and near IR spectrum and the other to IR. Also plotted in Fig. 4 is the distribution of spectral intensity for a black body at 1516 K.

The absorption of thermal radiation in the principal water vapor band at 2.6 μm and the CO_2 and water vapor band absorption at 4.3 μm are clearly seen. It can be readily seen that a 35 m diameter LNG fire is a grey body emitter with emissivity almost approaching unity (i.e., it is almost a black body).

4. Changes in measured spectra with burn time

A review of the 12 spectral scan data taken at 5 s intervals indicates the following:

1. The CO_2 emission in the 4.3 μm band dominates the emission in the early stages. As much as 45% of the total energy received by the spectrometer is accounted for by this band emission.
2. The soot emission gradually increases and dominates towards the end of the fire life. This may be due to the formation of increased quantity of luminous soot by the combustion of propane, butane, and ethane during the final stages of LNG fire. In this test series the LNG composition was 75% methane, 19% ethane and 4% propane.
3. The strong absorption bands (in the 2–2.6 μm range) due to an outer layer of hydrocarbons observed in the early spectral records disappear completely during the last 15 s of the burn. The first to disappear is propane followed by butane absorption at about 15 s before the end followed by ethane absorption. This is indicative of the complete combustion of these higher hydrocarbons at the end stages.
4. The relative importance of CO_2 emission and luminous soot emission received by the spectrometer as a function of time is shown in Fig. 4. The area under the measured spectral curve in the 1.5–4 μm is assumed to represent the radiance due to soot.[2] The area under the spectral curve for wavelengths greater than 4 μm is assumed to be due to CO_2. It is seen that the CO_2 emission, relative to that of soot emission, increases up to about 30 s; subsequently, the soot emission is higher.[3] A possible explanation for the sudden jump in soot emission is the sudden increase in soot particle formation due to the substantial release of ethane (and later propane) and significant decrease in methane emission from the LNG pool (due to fractional distillation of the liquid) at this time. Such a phenomenon has been observed in non-fire LNG boiling experiments conducted in a laboratory by Valencia-Chavez and Reid [12].

5. Estimation of soot temperature and emissivity

Except for the CO_2 band emission (at 4.3 μm) the rest of the energy received by the spectrometer can be assumed to be that due to emissions from luminous soot modified by the atmosphere. The moisture in the intervening atmosphere effectively absorbs all band emissions from water vapor in the fire. Inspection of the spectral data shown in Fig. 3 does not give direct information on soot emission, either the maximum apparent spectral intensity or the location of this maximum on the wavelength scale. Because the atmospheric transmissivity at 2.5 μm is close to 1 it is assumed that the measured intensity at this wavelength is the intensity at the fire surface at that wavelength. Assuming the luminous soot to be a grey body emitter several soot temperature emissivity combinations were evaluated to "fit" the observed intensity at 2.5 μm. The best fit resulted with a soot temperature of 1500 K and soot emissivity (independent of wavelength) of 0.14. This best fit is based on the assumption that the peak spectral radiance measured in the luminous soot emission is 4.27 kW/m^2 sr μm. This "fit", needless to state, is based on judgment and, hence, prone to errors. Recognizing this error, it can be argued the luminous soot temperature varies between 1300 and 1500 K and the corresponding emissivity varies from 0.23 to 0.14, respectively. Unfortunately, no definitive statements can be made since no independent measurements were made of the fire temperature or soot emissivity (by, say, grabbing samples from the fire and determining the soot density).

The calculated soot emissivity is somewhat greater than the value (of 0.1) suggested by Hottel and Sarofim [9] for the emissivity of luminous soot in a premixed methane flame in gas fired furnaces. It is possible that in a diffusion fire in the open the inefficiency of air mixing results in the conversion of a larger fraction of the fuel into carbon particles (soot) and, hence, higher soot emissivity.

[2] The choice of 4 μm as the upper limit for soot emission is somewhat arbitrary. However, since the purpose of this choice is to illustrate the relative variation in the emission strengths of CO_2 and soot, it is anticipated that the arbitrariness of the cut off wavelength will not affect the conclusions.

[3] A sudden jump was observed in the spectral intensity of the soot, by almost 50%, between a scan at 35 s into the burn and scan at 40 s. The visible flame as seen on the motion pictures did not exhibit any noticeable difference in its observable characteristics.

Table 4
Variation of estimated mean emissivity of soot with time for different (assumed) flame temperatures

Assumed flame temperature (K)	Calculated mean soot emissivity (ε_s) from spectral data at indicated times after ignition		
	15 s	20 s	40 s
1200	0.30	0.42	0.58
1300	0.20	0.28	0.39
1400	0.14	0.19	0.27
1500	0.10	0.14	0.19

The variation of calculated soot emissivity with burn time is given in Table 4 for different (assumed) flame temperatures. It is noticed that the soot emissivity increases with time. This is attributed to the burning of higher hydrocarbon fractions of the fuel at later stages of the burn. Ethane, propane and butane produce considerably more soot (expressed as mass of soot produced per unit mass of fuel burned) than methane. It should be noted that the aim of the spectrometer was on the lower sections of the fire. Had the center of view been at higher elevations in the fire the soot emissivity calculated through measured spectra would have been higher.It is also known that spectral emissivity of soot is dependent on wavelength [13], and is given by

$$\varepsilon_{\lambda,\text{soot}} = \varepsilon^* \lambda^{-0.77} \quad (1)$$

where

ε^* = a constant with units of $(\mu m)^{0.77}$

In the above case to match the observed spectrum in the 2–2.5 μm range with the maximum soot spectral radiance of 4.27 kW/m^2 sr μm, it is necessary to adjust the temperature to 1300 K and the value of ε^* to 0.49 $(\mu m)^{0.77}$. In the 1.5–5.5 μm range, then the average emissivity of soot becomes 0.204. An assumption of flame temperature of 1500 K and the emissivity variation given by Eq. (1) leads to the calculated spectral radiant intensity for soot that does not agree with the measured spectral data. In a later section it is shown that lower temperature assumption is not consistent with measured energy received in the 4.3 μm band for CO_2 emission and physically possible CO_2 partial pressures in the fire. Hence the only conclusion that can be drawn is that the soot emissivity in this fire may not follow the emissivity variation with wavelength given by Eq. (1).

6. Emissive power of the fire

The emissive power of that part of the fire seen by the spectrometer is estimated primarily from the information contained in the 4.3 μm CO_2 band. The calculation is based on the principle of estimating the partial pressure-path length product (pL) for CO_2 in the flame by using the observed emission energy. The emission from the flame in this band is calculated by measur-

Table 5
Calculated emissivity of CO_2 in the 4.3 mm band and the estimated pL for CO_2 in the flame

Assumed flame temperature (K)	Black body emissive power (kW/m^2)	Ratio of band energy flux received to black body emissive power[a] ($\times 10^{-2}$)	Atmospheric absorptivity at 4.3 μm band for 236 m distance[b] ($\alpha_{4.3}$) ($\times 10^{-2}$)	Calculated[b] band emissivity at 4.3 μm band ($\varepsilon_{4.3}$) ($\times 10^{-2}$)	Calculated [b] partial pressure-path length product for CO_2, pL_{CO_2} (atm m)	Partial pressure of CO_2 in the flame[c], P_{CO_2} (atm)	Remarks
1300	161.9	7.35	3.29	10.64	17.49	1.35	The value of P_{CO_2} calculated is not physically valid because for stoichiometric combustion of methane in air P_{CO_2} is 0.095 atm. All calculated P_{CO_2} must be lower than the stoichiometric value
1400	217.8	5.46	3.01	8.47	2.91	0.22	
1500	287.0	4.15	2.74	6.89	1.01	0.08	Physically acceptable value for P_{CO_2}. The % excess air in the fire is calculated to be 21%[d]

It is not known what amount of excess air was present in the fire at the aim of the spectrometer, Depending upon excess air amount over and above the calculated value above, the partial pressure of CO_2, will be lower leading to higher predicted flame temperature.

[a] Energy received is estimated to be 11.9 kW/m^2 at the spectrometer position.

[b] See Raj et al. [6].

[c] Calculated based on the assumption of a path length of 13 m (diameter of the fire).

[d] Percent excess air (above stoichiometric requirement) = $100 \times [0.105/P_{CO_2} - 1.105]$.

Table 6
Calculated flame emissive power

Assumed flame temperature (K)	Black body emissive power, E_B (kW/m^2)	Calculated[a] partial pressure − path length of CO_2 in the flame for stoichiometric combustion $P_{CO_2}L$, (atm m)	Calculated[b] partial pressure − path length of H_2O vapor $P_{H_2O}L$, (atm m)	Total emissivity of each specie[c]					Flame emissive power[f], E (kW/m^2)
				ε_{CO_2}	ε_{H_2O}	Band overlap correction, $\varepsilon_{(CO_2-H_2O)}$	ε_{soot}[d]	ε_{total}[e]	
1500	287.0	1.24	2.74	0.19	0.35	0.07	0.14	0.61	175

[a] Path length through the fire is assumed to be 13 m (diameter).
[b] $P_{H_2O}L = 2\ P_{CO_2}L$.
[c] ε_{CO_2} is calculated with $P_{CO_2}L = 1.24$ atm m and using the charts in Hottel and Sarofim [9].
[d] ε_{soot} is the calculated emissivity of soot (see section on soot temperature and emissivity).
[e] $\varepsilon_{total} = \varepsilon_{CO_2} + \varepsilon_{H_2O} - \varepsilon_{(CO_2-H_2O)} + \varepsilon_{soot}$.
[f] $E = \varepsilon_{total}E_B$.

ing the energy received in the 4.3 μm band and the atmospheric transmissivity in this band for the distance of the spectrometer. With an assumed flame temperature and the calculated 4.3 μm band emission energy the band emissivity is determined. With this value of band emissivity and the published relationship between band emissivity and $(pL)_{CO_2}$ the latter value is calculated. Once this is accomplished the total emissivities of CO_2 and H_2O vapor are obtained from Hottel charts [9]. The true flame emissive power is then calculated by knowing the blackbody emissive power (for the assumed temperature), the soot emissivity and the total band emissivities of CO_2 and H_2O.

The calculation of the CO_2 partial pressure in the flame from the known 4.3 μm CO_2 band energy received by the spectrometer and the assumed flame temperature is a tedious procedure. Details are presented by Raj et al. [6]. The calculation methodology is, in part, an inverse procedure to that developed by Edwards and Balakrishnan [14] for estimating the total emissivities of gases from known pL values for individual species and the temperature of the gases. The result of these calculations is indicated in Table 5. It is seen that the only physically acceptable solution to the flame temperature which is consistent with the measured spectral energy received by the spectrometer at 4.3 μm band is close to 1500 K.

Table 6 shows the calculated values for the emissivity of the 13 m diameter LNG fire (emissivity = 0.61), assuming stoichiometric combustion at the lower parts of fire. The emissivity is substantially lower than unity and therefore this 13 m diameter fire has to be considered as being not optically thick. It is also noticed that a substantial part of the contribution to the total emissivity comes from the water vapor and CO_2. The calculated value for the mean emissive power (175 kW/m^2) agrees remarkably closely with the value obtained from the narrow angle radiometer (view angle 7°), which was aimed at about the same location in the fire as the spectrometer was. The flame emissive power data from the narrow angle radiometer (uncorrected for atmospheric absorption) varied between 160 and 180 kW/m^2 during the first 40 s after ignition; the measured value at 20 s was 175 kW/m^2. The atmosphere absorption corrected narrow angle radiometer value will be therefore higher than this value at 20 s by about a 10% factor.

The spectral emission data obtained in the 35 m diameter LNG fire test at Montoir are shown in Fig. 5. Also indicated in this figure for comparison is the spectrum from a blackbody at a temperature of 1516 K. This temperature was chosen so that the spectral radiance measured at 2.26 μm (which was the maximum value for the data measured) would be equal to the blackbody spectral radiance at the same wavelength. This is based on the assumption that the atmospheric absorption at ∼21 m from the fire surface at 2.26 μm wavelength is negligible and the measured data thus represents the "fire surface" spectral radiance.

The results presented in Fig. 5 indicate that the emission from the fire essentially tracks the black body curve, except in the 2.75 μm H_2O band and in the 4.3 μm CO_2 band, where the absorption is nearly total even for the relatively short path length of ∼21 m and atmospheric conditions of 54% relative humidity and 21 °C temperature. This figure further indicates that the luminous soot has a high emissivity; and, the total emissivity due to the emissivity of luminous soot and band emissions from H_2O and CO_2 in the fire is slightly less than but close to unity. This is in contrast to the emission from the 13 m China Lake fire LNG fire whose soot emissivity was estimated to be 0.14 and the overall fire emissivity was calculated to be 0.61 [see Table 5]. This implies that the Montoir fire (35 m diameter) was essentially an optically thick emitter whereas the China Lake fire was not optically thick. It can be postulated, therefore, that the optical thickness of a LNG fire lies somewhere between 20 and 35 m.

It is interesting to note that the equivalent blackbody radiative temperatures of the 13 m diameter China Lake LNG pool fire on water and the 35 m diameter Montoir LNG pool fire on land are practically the same (1500 and 1516 K, respectively) within the estimated uncertainty in determining the fire emission after correcting for the absorption in the intervening atmosphere. The black body emissive power corresponding to 1516 K temperature is 300 kW/m^2. While the Montoir 35 m diameter fire was highly radiative in the lower burning regions (with an effective black body temperature of 1516 K and emissivity of unity), the overall mean emissive power (based on a description of the fire as a cylinder and height given by Thomas' correlation) was calculated to be 165 kW/m^2 [8]. This is compared to the calculated mean emissive power value of 175 kW/m^2 for the 13 m diameter China Lake fire. The reason that the 35 m diameter fire seems to have lower overall heat flux emission rate is due to the formation of black smoke (due to oxygen starvation in the core sections

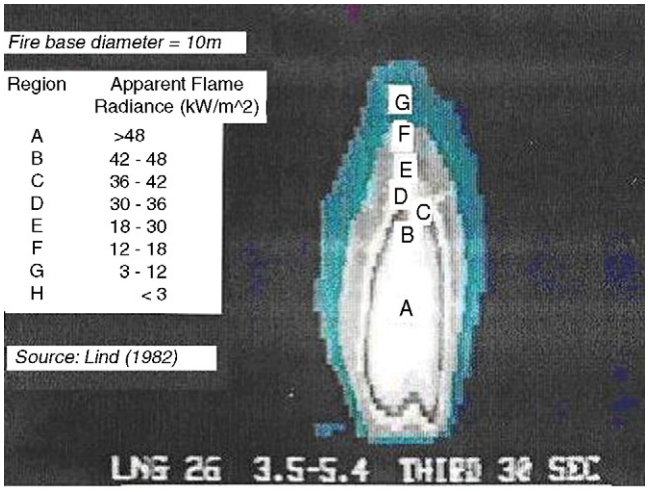

Fig. 6. Infrared scan map in 3.5–5.4 μm of a 10 m dia LNG pool fire on water.

of the larger fire and the resultant incomplete combustion of vapors).

Images in Figs. 6 and 7 show different magnitude infrared emission regions (represented by different colors) from a 10 m diameter LNG pool fire [7]. These images were obtained using a scanning infrared device with a 15 s averaging time. The images presented are respectively for the 3.5–5.4 μm band and 8.2–11.7 μm band without correcting for the atmospheric absorption. The figures indicate that the most emissive part of the fire is about half way up its visible height and not close to the base. It is not possible to infer from these data whether the fire was optically thick and if so in what regions. No cold vapor core can be discerned either. Since no scans were made at other wavelengths (for example, in the 1.5–3.5 μm) it is difficult to use the emissive power data shown in Figs. 6 and 7 to calculate the overall (mean) emissive power of the fire.

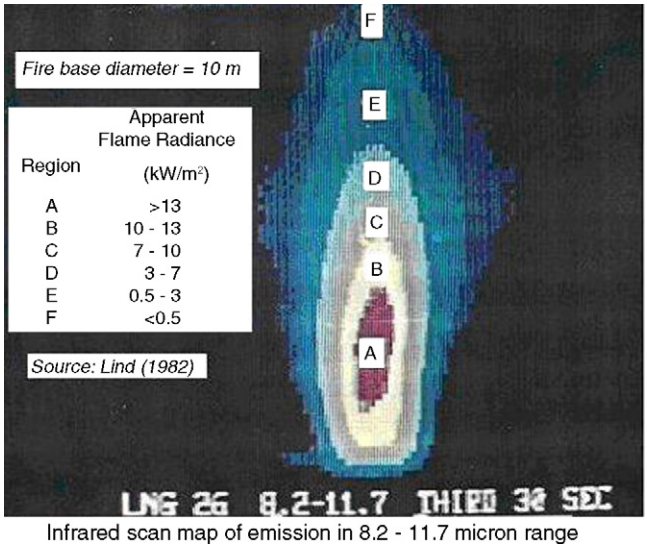

Fig. 7. Infrared scan map in 8.2–11.7 μm of a 10 m diameter LNG pool fire on water.

7. Conclusions

The following conclusions are reached from the analysis of the LNG pool fire spectral data discussed in this paper.

1. The emission spectrum measured in the 13 m diameter LNG pool fire indicates that significant emission occurs in the H_2O and CO_2 bands. Water vapor emission constitutes about 50% of the total emission, 25% from carbon dioxide and the remainder from luminous soot. At later stages of the fire when higher hydrocarbon molecules are burning the fraction of energy emitted by soot increases by 10–20%.
2. The mean flame temperature cannot be determined precisely, but it is in the range 1300–1500 K. The calculations based on 4.3 μm CO_2 band emission indicate that the temperature is probably closer to 1500 K. The spectral data from the 35 m diameter fire indicates that the lower regions of the fire can be represented as a blackbody emitter at 1516 K.
3. Estimated soot emissivity for the 13 m diameter fire during the major part of burning time is in the 0.14–0.19 range (for the 13 m diameter LNG fire). These are lower than 0.5–0.6 reported in the AGA tests. For the 35 m diameter fire the soot emissivity is close to unity.
4. The mean emissive power of the 13 m diameter fire calculated using the emission spectrum of the 4.3 μm CO_2 band is 175 kW/m^2. This value is close to the apparent value measured by narrow angle radiometer at the same time after ignition as the spectral scan. However the "true" emissive power measured by the narrow angle radiometer will be higher by about 10% when the atmospheric attenuation is accounted for.
5. For a given distance the atmospheric transmissivity for LNG flame radiation is much lower than for radiation from a black body at the same temperature. This is because of the band emission from H_2O and CO_2 in LNG fires and the strong absorption of this emission by the same species in the atmosphere.
6. While a model describing LNG fire emission in terms of soot, water vapor and carbon dioxide emissivities should provide an improved description of the radiation from the fire, not enough spectral data exist to define, precisely, the characteristics parameters in the model in terms of the burning rate and the size of the fire. The key parameters such as soot density and the rate of production of soot are not yet available on which to base such a model.
7. LNG fire internal temperature from the 13 m diameter fire on water and the 35 m diameter fire on land seem to be close to 1500 K.
8. A 35 m diameter LNG fire is almost a blackbody radiator in the highest thermal output regions (lower regions of the fire). That is, 35 m diameter fire may represent an optically thick fire.

References

[1] GRI, LNG fires—combustion and radiation, in: P.K. Raj (Ed.), Proceedings of the Joint MIT-GRI LNG Safety and Research Workshop, March

22–24, Published by Gas Research Institute, 8600 West Bryn Mawr Avenue, Chicago, IL, 1982, p. 60631.
[2] Sandia, in: M. Hightower, L. Gritzo, A. Luketa-Hanlin, J. Covan, S. Tieszen, G. Wellman, M. Irwin, M. Kaneshige, B. Melof, C. Morrow, D. Ragland (Eds.), Guidance on Risk Analysis and Safety Implications of a Large Liquefied Natural Gas (LNG) Spill Over Water, Sandia National Laboratory Rep. #SAND2004-6258, U.S. Department of Energy, Washington, DC, 2004.
[3] M. Considine, Thermal Radiation Hazard Ranges from Large Hydrocarbon Pool Fires," Report #SRD R297, Safety and Reliability Directorate, UK Atomic Energy Authority, Wigshaw Lane, Culcheth, Warrington, WA3 4NE, UK, October 1984.
[4] P.K. Raj, Large LNG fire thermal radiation—modeling issues and hazard criteria revisited, Process Safe. Progress 24 (3) (2005) 192–202.
[5] AGA, LNG Safety Program, Interim Report on Phase II Work, IS-3-1, Section H, Published by the American Gas Association, Washington, DC, July 1974.
[6] P.K. Raj, A.L. Moussa, K. Aravamudan, Experiments Involving Pool and Vapor Fires from Spills of LNG on Water, NTIS #AD-A077073, USCG Report, Washington, DC, 20590, 1979.
[7] D.C. Lind, Recent LNG pool fire and vapor fire tests at China lake, in: P.K. Raj (Ed.), MIT-GRI LNG Safety and Research Workshop Proceedings, Published by Gas Research Institute, vol. III, Chicago, IL, 1982.
[8] D.J. Nedelka, J. Moorehouse, R.F. Tucker, The Montoir 35 m diameter LNG pool fire experiments, in: TRCP.3148R, Proceedings of the Ninth International Conference and Expo on LNG, LNG IX, Nice, France, 1989.
[9] H.C. Hottell, S.A. Sarofim, Radiative Transfer, McGraw Hill Publications, New York, NY, 1967.
[10] W.L. Wolfe (Ed.), Handbook of Military Infrared Technology, Office of Naval Research, Department of Navy, Washington, DC, 1965.
[11] H. Malvos, P.K. Raj, Details of 35 m diameter LNG fire tests conducted in montoir, France in and analysis of fire spectral and other data, in: Paper Presented at the AIChE 2006 Spring National Meeting, Orlando, FL, April 23–27, 2006.
[12] J.A. Valencia-Chavez, R.C. Reid, The Effect of Composition on Boiling Rates of Liquefied Natural Gas for Confined Spills on Water, LNG Research Center report, M.I.T., Cambridge, MA, 1978.
[13] D. Burgess, M. Hertzberg, in: N.H. Afghan, J.M. Beer (Eds.), Radiation from Pool Fires, Heat Transfer in Flames, Scripta Boob Co., Washington, DC, 1974.
[14] D.K. Edwards, A. Balakrishnan, Thermal radiation by combustion gases, Int. J. Heat Mass Trans. 16 (1) (1973) 25–40.